Journal of Porphyrins and Phthalocyanines
J. Porphyrins Phthalocyanines 2015; **19**: 1–12
DOI: 10.1142/S1088424615500832

Published at http://www.worldscinet.com/jpp/

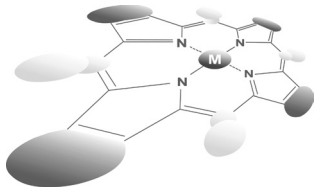

The effect of substitutents at alkylsulfanyl/arylsulfanyl non-peripherally substituted phthalocyanines: Spectral and photophysical properties, basicity and photostability

Antonin Cidlina[a], Zuzana Pausimova[b], Miroslav Miletin[a], Petr Zimcik[a◊] and Veronika Novakova*[b◊]

[a] *Department of Pharmaceutical Chemistry and Drug Control, Faculty of Pharmacy in Hradec Kralove, Charles University in Prague, Heyrovskeho 1203, Hradec Kralove, Czech Republic*
[b] *Department of Biophysics and Physical Chemistry, Faculty of Pharmacy in Hradec Kralove, Charles University in Prague, Heyrovskeho 1203, Hradec Kralove, Czech Republic*

Received 7 June 2015
Accepted 16 July 2015

ABSTRACT: A series of magnesium, zinc and metal-free derivatives of non-peripherally substituted phthalocyanines (Pcs) bearing alkylsulfanyl or arylsulfanyl groups of different bulkiness was synthesized. Their spectral and photophysical properties including also the basicity of azomethine nitrogens and photostability were compared within the series as well as with similar peripherally substituted Pcs. Non-peripheral position of substituents led to the 70 nm red-shift of Q-band in comparison to the peripherally substituted Pcs. However, unexpected blue-shift of approximately 50 nm was observed in the series of non-peripherally substituted Pcs for the most bulky *tert*-butylsulfanyl derivative caused probably by extreme distortion of the macrocycle. The substitution had no effect on photophysical properties and compounds reached Φ_Δ values 0.74–0.76 and Φ_F 0.053–0.080 for zinc complexes, and Φ_Δ 0.47–0.51 and Φ_F 0.10–0.17 for magnesium complexes following the rule of heavy atom effect. Generally, non-peripherally substituted Pcs possessed improved singlet oxygen production in comparison to peripherally substituted ones. The photostability of the target compounds decreased with the red-shift of their absorption maxima with the arylsulfanyl derivatives being less photostable. The basicity of azomethine nitrogens was clearly dependent on the position and the character of substituent. Thus, non-peripherally substituted Pcs showed extraordinary increased basicity over the peripherally substituted ones with the most pronounced effect at alkylsulfanyl derivatives.

KEYWORDS: phthalocyanine, non-peripheral substitution, singlet oxygen, fluorescence, basicity, photobleaching.

INTRODUCTION

Phthalocyanines (Pcs) are intensively colored synthetic dyes structurally close to porphyrins with interesting spectral, electrochemical and photophysical properties. Due to extended 18 π-conjugated macrocyclic system, they absorb the light in red region beyond 650 nm. Their application can be found in various fields, such as photodynamic therapy of cancer [1–4], solar cells [5], gas sensors [6], organic light emitting devices [7] or near infrared fluorescence imaging probes [8]. The near infrared absorption brings advantages in many of these applications especially due to limited spectral competition with other molecules (endogenous chromophores present in biological material) and lower light scattering.

The position of the Pcs main absorption band (*i.e.* the Q-band) can be manipulated by annulation of additional benzene rings forming, thus, Pcs homologs (*e.g.* naphthalocyanines [9]), by nature and position of peripheral substituents [10], and partially also by

◊ SPP full member in good standing

*Correspondence to: Veronika Novakova, email: veronika.novakova@faf.cuni.cz, tel: +420 495067380, fax: +420 495067167

coordination of different metal cations into the center [11]. However, higher homologs of Pcs with stronger π–π interactions suffer usually from increased aggregation and low solubility leading to the loss of optimal spectral and photophysical properties. Evidently, the modulation of the position and character of substituents is the most effective way for tuning spectral properties of Pcs. Hence, pronounced bathochromic shift of Q-band was achieved by substitution in non-peripheral positions (1,4,8,11,15,18,22,25) of Pc core [11, 12]. Heteroatom connecting peripheral substituent to the macroclic core can contribute to the π-electron system shifting, thus, absorption more to the red part. Accordingly, alkylsulfanyl or arylsulfanyl substituents are known to bathochromically shift the Q-band due to efficient overlapping of its 3*p* orbitals with *p*-orbitals of Pc [13]. Further, it has been systematically demonstrated that slight distortion of the macrocycle caused by non-peripheral substitution leads to significant red-shift of Q-band. This was shown on Pcs bearing different substituents (*i.e.* alkyl/aryl- [14], alkyloxy/aryloxy [9] as well as alkylsulfanyl/arylsulfanyl [11] derivatives) and proved experimentally as well as by theoretical calculations [15, 16]. Moreover, the substitution in non-peripheral positions of the macrocycle is known to reduce unfavorable aggregation behavior [17, 18].

Combining above-mentioned knowledge, the target magnesium non-peripherally substituted Pc with bulky alkylsulfanyl groups (**3Mg**, Chart 1) was designed. Surprisingly, unexpected blue shift was observed (data shown below). That was why, the series was enlarged to the other compounds **1M**, **2M**, **4M** and **5M** (Chart 1) of different bulkiness and alkylsulfanyl- or arylsulfanyl-nature of substituent to explain this feature. Metal complexes as well as corresponding metal free derivatives were included in the study. Only recently, Dumoulin and co-workers [19] described similar blue shift comparing two metal-free Pcs bearing *tert*-butylsulfanyl and hexylsulfanyl groups attached in non-peripheral positions and attributed it to the substantially increased distortion of the former macrocycle based on X-ray structures and theoretical calculations. In this work, series of compounds enabling clear comparison of alkylsulfanyl *vs.* arylsulfanyl substitution of different bulkiness was designed. Besides spectral properties, photophysical evaluation, basicity of azomethine nitrogens as well as photostability will be of interest in present work.

EXPERIMENTAL

General

All of the organic solvents used in the syntheses were of analytical grade. Anhydrous butanol for the cyclotetramerization was freshly distilled from magnesium, anhydrous quinoline was dried over calcium hydride and distilled under reduced pressure. An anhydrous DMF was purchased from Sigma-Aldrich. Unsubstituted zinc phthalocyanine (ZnPc) was purchased from Sigma-Aldrich. All of the other chemicals for the syntheses were purchased from certified suppliers (*i.e.* Sigma-Aldrich, TCI Europe, Acros, and Merck) and used as received. TLC was performed on Merck aluminum sheets coated with silica gel 60 F254. Merck Kieselgel 60 (0.040–0.063 mm) was used for column chromatography. The melting points were measured on an Electrothermal IA9200-series digital melting-point apparatus (Electrothermal Engineering, Southend-on-Sea, Essex, Great Britain). The infrared spectra were measured on a Nicolet

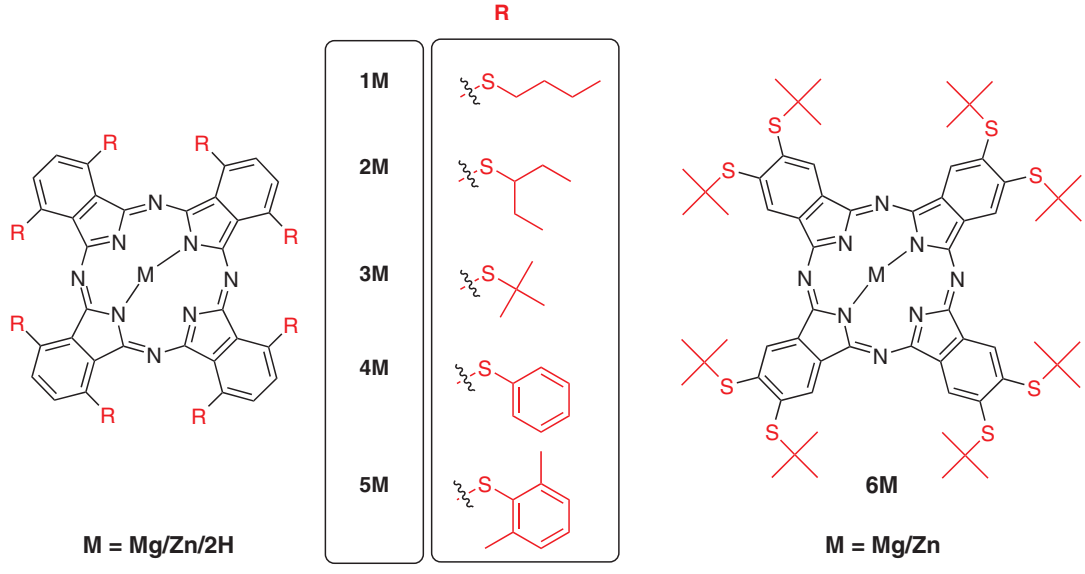

Chart 1. Structures of investigated compounds **1M–6M**

6700 spectrometer in ATR mode. The ^{1}H and ^{13}C NMR spectra were recorded on a Varian Mercury Vx BB 300 NMR spectrometer or VNMR S500 NMR spectrometer. The chemical shifts are reported relative to $Si(CH_3)_4$ and were locked to the signal of the solvent. The UV-vis spectra were recorded using a Shimadzu UV-2600 spectrophotometer. The steady-state fluorescence spectra were measured using an AMINCO-Bowman Series 2 luminescence spectrometer. The MALDI-TOF mass spectra were recorded in positive reflectron mode on a 4800 MALDI TOF/TOF mass spectrometer (AB Sciex, Framingham, MA, USA) in *trans*-2-[3-(4-*tert*-butylphenyl)-2-methyl-2-propenylidene]-malononitrile, which was used as a matrix. The instrument was calibrated externally with a five-point calibration using a Peptide Calibration Mix1 kit (LaserBio Laboratories, Sophia-Antipolis, France). 3,6-Bis(pentan-3-ylsulfanyl) phthalonitrile (**2**) [20], 3,6-bis(*tert*-butylsulfanyl)phthalonitrile (**3**) [21], 3,6-bis(phenylsulfanyl)phthalonitrile (**4**) [11], 3,6-bis(adamantan-1-ylsulfanyl)phthalonitrile (**7**) [22], 2,3-dicyano-1,4-phenylene bis(4-methylbenzenesulfonate) (**8**) [23] and the reference compounds **6Mg**, **6Zn** [24] were prepared according to previously published procedures. The compound 3,6-bis(butylsulfanyl)phthalonitrile (**1**) [10], 3,6-bis[(2,6-dimethylphenyl)sulfanyl] phthalonitrile (**5**) [12] were prepared with a minor modification described below. Our analytical data for previously published compounds corresponded well with those reported.

Synthesis of precursors

3,6-Bis(butylsulfanyl)phthalonitrile (1). The finely ground anhydrous potassium carbonate (5.3 g, 38.4 mmol) was sonicated in DMSO (50 mL) for 30 min and then butanethiol (2.9 g, 32.0 mmol) was added. Later, the compound **8** (6 g, 12.8 mmol) was added to the mixture in six portions during the next 2 h and stirring continued for next 16 h at room temperature. The reaction was then quenched by water (150 mL). The mixture was extracted with ethyl acetate (3 × 40 mL). The combined organic layers were dried over anhydrous Na_2SO_4 and solvent was removed under reduced pressure. The crude product was purified by column chromatography on silica with toluene as the mobile phase (R_f = 0.27). Yield 2.32 g (59%) of light yellow solid. ^{1}H NMR (300 Hz, $CDCl_3$): δ, ppm 7.86 (s, 2H, ArH), 3.38 (t, J = 7 Hz, 4H, SCH_2), 2.02 (quint, J = 7 Hz, 4H, SCH_2CH_2), 1.91–1.75 (m, 4H, CH_2CH_3), 1.30 (t, J = 7 Hz, 6H, CH_3). ^{13}C NMR (75 Hz, $CDCl_3$): δ, ppm 141.3, 132.0, 117.0, 113.8, 33.4, 30.6, 21.4, 13.5.

3,6-Bis(pentan-3-ylsulfanyl)phthalonitrile (2). ^{1}H NMR (300 Hz, $CDCl_3$): δ, ppm 7.9 (s, 2H, ArH), 3.59 (quint, J = 6 Hz, 2H, CH), 2.14–1.92 (m, 8H, CH_2), 1.39 (t, 12H, CH_3). ^{13}C NMR (75 Hz, $CDCl_3$): δ, ppm 141.2, 134.2, 118.8, 114.1, 52.9, 26.6, 11.0.

3,6-Bis(*tert*-butylsulfanyl)phthalonitrile(3). ^{1}H NMR (300 Hz, $CDCl_3$): δ, ppm 8.18 (s, 2H, ArH), 1.76 (s, 18H, CH_3). ^{13}C NMR (75 Hz, $CDCl_3$): δ, ppm 140.8, 139.7, 125.0, 114.8, 50.5, 31.0.

3,6-Bis(phenylsulfanyl)phthalonitrile (4). ^{1}H NMR (300 Hz, $CDCl_3$): δ, ppm 7.92–7.72 (m, 10H, ArH), 7.32 (s, 2H, ArH). ^{13}C NMR (75 Hz, $CDCl_3$): δ, ppm 142.8, 134.5, 132.2, 130.2, 130.0, 129.6, 115.1, 113.6.

3,6-Bis[(2,6-dimethylphenyl)sulfanyl]phthalonitrile (5). The finely ground anhydrous potassium carbonate (235 mg, 1.7 mmol) was sonicated in anhydrous DMSO (10 mL) for 30 min and then 2,6-dimethylbenzenethiol (120 mg, 0.85 mmol) was added. Later, compound **8** (100 mg, 0.21 mmol) was added in one portion and the stirring continued for next 16 h at room temperature. The reaction was then quenched by water (50 mL). The mixture was extracted with ethyl acetate (3 × 15 mL). The combined organic layers were dried over anhydrous Na_2SO_4 and solvent was removed under reduced pressure. The crude product was purified by column chromatography on silica with toluene/chloroform (5:1) as the mobile phase (R_f = 0.40). Yield 63 mg (74%) of yellow solid. ^{1}H NMR (300 Hz, $CDCl_3$): δ, ppm 7.61–7.58 (m, 2H, ArH), 7.52 (d, J = 7 Hz, 4H, ArH), 6.76 (s, 2H, ArH) 2.71 (s, 12H, CH_3). ^{13}C NMR (75 Hz, $CDCl_3$): δ, ppm 144.0, 141.7, 130.7, 129.0, 128.9, 127.1, 113.7, 113.4, 21.7.

3,6-Bis(adamantan-1-ylsulfanyl)phthalonitrile (7). The finely ground anhydrous potassium carbonate (8.2 g, 59 mmol) was sonicated in DMSO (50 mL) for 30 min and then 1-adamantanethiol (5 g, 30 mmol) was added. Later, compound **8** (2.78 g, 6 mmol) was added to the mixture in six portions during the next 1h and the stirring was continued for 16 h at room temperature. The reaction was then quenched by water (150 mL). The mixture was extracted with chloroform (4 × 40 mL). The combined organic layers were dried over anhydrous Na_2SO_4 and solvent was removed under reduced pressure. The crude product was purified by column chromatography on silica with toluene and further with toluene/chloroform (1:1) (R_f = 0.41) as the mobile phase. Yield 2.76 g (96%) of white solid. ^{1}H NMR (500 Hz, $CDCl_3$): δ, ppm 8.12 (s, 2H, ArH), 2.44 (s, 6H, CH_2), 2.30–2.25 (m, 12H, $CH + CH_2$), 2.01 (q, 12H, $CH + CH_2$). ^{13}C NMR (125 Hz, $CDCl_3$): δ, ppm 141.1, 137.7, 125.3, 115.0, 53.2, 43.7, 35.8, 30.1.

Synthesis of macrocycles

General procedure for synthesis of magnesium (II) complexes. Magnesium turnings (10 eq.) and a small crystalline of iodine were refluxed in freshly distillated anhydrous butanol (10–50 mL) for 3 h. Later, the compound **1–5** (1 eq.) was added and reflux continued for next 24 h. The reaction mixture was cooled down and solvent was removed under reduced pressure. The aqueous solution of acetic acid (50%) (v/v) was added (about 100 mL) and the mixture was stirred at room temperature for 1 h. Precipitate was collected by filtration

and washed with water. Purification of the product is mentioned at each compound below.

1,4,8,11,15,18,22,25-Octakis(butylsulfanyl)phthalocyaninato magnesium (II) (1Mg). The compound **1Mg** was prepared from **1** (1 g, 3.28 mmol) according to general procedure for synthesis of magnesium complexes. The crude product was washed thoroughly with methanol and purified by column chromatography on silica with toluene/chloroform/THF (40:4:1) as a mobile phase (R_f = 0.32). Yield 722 mg (70%) of dark green solid. UV-vis (THF): λ_{max}, nm (log ε) 776 (5.26), 694 (4.62), 501 (sh), 359 (4.68). ^{1}H NMR (300 Hz, $CDCl_3$/pyridine-d_5): δ, ppm 7.93 (broad s, 8H, ArH), 3.48 (broad s, 16H, SCH_2), 2.14 (quint, *J* = 7 Hz, 16H, SCH_2CH_2), 1.92–1.70 (m, 16H, CH_2CH_3), 1.16 (t, *J* = 7 Hz, 24H, CH_3). ^{13}C NMR (75 Hz, $CDCl_3$/pyridine-d_5): δ, ppm 153.5, 132.7, 124.8, 32.11, 31.3, 23.1, 14.1. IR: ν_{max}, cm^{-1} 2956, 2929, 2870, 1561, 1463, 1436, 1319, 1284, 1210, 1107, 1084, 926. MS (MALDI): *m/z* 1240.3 $[M]^+$.

1,4,8,11,15,18,22,25-Octakis(pentan-3-yl)phthalocyaninato magnesium (II) (2Mg). The compound **2Mg** was prepared from **2** (500 mg, 1.51 mmol) according to general procedure for synthesis of magnesium complexes. The crude product was washed thoroughly with methanol and purified by column chromatography on silica with toluene/THF (20:1) as the mobile phase (R_f = 0.75). Yield 220 mg (43%) of dark brown solid. UV-vis (THF): λ_{max}, nm (log ε) 774 (5.22), 692 (4.60), 505 (sh), 363 (4.66). ^{1}H NMR (500 Hz, $CDCl_3$): δ, ppm 7.94 (s, 8H, ArH), 3.76–3.63 (m, 8H, CH), 2.14–1.98 (m, 32H, CH_2), 1.25 (t, *J* = 7 Hz, 48H, CH_3). ^{13}C NMR (125 Hz, $CDCl_3$): δ, ppm 153.2, 136.5, 132.9, 131.8, 130.8, 128.6, 126.7, 50.0, 27.1, 12.1. IR: ν_{max}, cm^{-1} 2964, 1931, 1872, 1558, 1491, 1461, 1377, 1318, 1281, 1205, 1139, 1106, 919. MS (MALDI): *m/z* 1352.4 $[M]^+$, 1375.4 $[M + Na]^+$, 1391.1 $[M + K]^+$.

1,4,8,11,15,18,22,25-Octakis(*tert*-butylsulfanyl)phthalocyaninato magnesium (II) (3Mg). The compound **3Mg** was prepared from **3** (200 mg, 0.66 mmol) according to general procedure for synthesis of magnesium complexes. The crude product was purified by column chromatography on silica with chloroform/THF (10:1) as a mobile phase (R_f = 0.41). The pure **3Mg** was washed thoroughly with methanol. Yield 63 mg (31%) of dark green solid. UV-vis (THF): λ_{max}, nm (log ε) 724 (5.08), 657 (4.44), 467 (sh), 375 (4.58). ^{1}H NMR (300 Hz, $CDCl_3$/pyridine-d_5): δ, ppm 8.26 (s, 8H, ArH), 1.62 (s, 144H, CH_3) ^{13}C NMR (75 Hz, $CDCl_3$/pyridine-d_5): δ, ppm 152.4, 142.5, 139.9, 139.5, 137.2, 134.5, 133.3, 132.2, 41.5, 31.4. IR: ν_{max}, cm^{-1} 2962, 2918, 2894, 2861, 1689, 1553, 1459, 1389, 1362, 1128, 1096, 917, 783. MS (MALDI): *m/z* 1240.3 $[M]^+$.

1,4,8,11,15,18,22,25-Octakis(phenylsulfanyl)phthalocyaninato magnesium (II) (4Mg). The compound **4Mg** was prepared from **4** (500 mg, 1.64 mmol) according to general procedure for synthesis of magnesium complexes. The crude product was purified by column chromatography on silica with toluene/THF (30:1) as a mobile phase (R_f = 0.33). Yield 308 mg (61%) of dark brown solid. UV-vis (THF): λ_{max}, nm (log ε) 775 (5.35), 695 (4.71), 495 (sh) 361 (4.80). ^{1}H NMR (300 Hz, $CDCl_3$/pyridine-d_5): δ, ppm 7.75 (broad s, 16H, ArH), 7.59–6.84 (m, 32H, ArH). No signal was detected in ^{13}C NMR spectrum. IR: ν_{max}, cm^{-1} 3056, 2785, 2538, 1957, 1884, 1582, 1557, 1475, 1461, 1439, 1320, 1287, 1177, 1107, 918, 791. MS (MALDI): *m/z* 1400.1 $[M]^+$.

1,4,8,11,15,18,22,25-Octakis(2,6-dimethylphenylsulfanyl)phthalocyaninato magnesium (II) (5Mg). The compound **5Mg** was prepared from **5** (286 mg, 0.71 mmol) following the general procedure for synthesis of magnesium complexes. The crude product was purified by column chromatography on silica with a toluene/THF (50:1) as a mobile phase (R_f = 0.50). The pure compound was washed thoroughly with methanol. Yield 179 mg (47%) of dark brown solid. UV-vis (THF): λ_{max}, nm (log ε) 788 (5.38), 702 (4.72), 501 (sh), 360 (4.81). ^{1}H NMR (300 Hz, $CDCl_3$/pyridine-d_5): δ, ppm 7.36–7.28 (m, 24H, ArH), 6.88 (s, 8H, ArH), 2.64 (s, 48H, CH_3). ^{13}C NMR (75 Hz, $CDCl_3$/pyridine-d_5): δ, ppm 144.5, 139.1, 131.4, 130.7, 129.4, 128.8, 124.4, 22.2. IR: ν_{max}, cm^{-1} 3054, 2952, 1561, 1459, 1377, 1212, 1166, 1107, 1053, 988, 916, 517, 769. MS (MALDI): *m/z* 1624.2 $[M]^+$.

General procedure for synthesis of metal-free derivatives. The compound **1Mg**, **2Mg**, **4Mg** or **5Mg** (1 eq.) was dissolved in THF (40 mL) and *p*-toluenesulfonic acid (TsOH) was added (7 eq.). The reaction mixture was stirred at room temperature for 1 h protected from light by aluminum foil. Later, the reaction was quenched by water (50 mL) and precipitate was collected by filtration. The crude product was washed with water and thoroughly with methanol. The product was purified by column chromatography on silica (mobile phases are mentioned at each compound below) and thoroughly washed with methanol.

1,4,8,11,15,18,22,25-Octakis(butylsulfanyl)phthalocyanine (1H). The compound **1H** was prepared from **1Mg** (90 mg, 0.072 mmol) according to the general procedure for synthesis of metal-free derivatives. Mobile phase: chloroform (R_f = 0.65). Yield 52 mg (59%) of green solid. UV-vis (THF): λ_{max}, nm (log ε) 805 (5.18), 718 (4.61), 523 (sh), 350 (4.71). ^{1}H NMR (300 Hz, $CDCl_3$/pyridine-d_5): δ, ppm 7.56 (s, 8H, ArH), 3.21 (broad s, 16H, SCH_2), 1.97–1.81 (m, 16H, SCH_2CH_2), 1.78–1.61 (m, 16H, CH_2CH_3), 1.09 (t, *J* = 7 Hz, 24H, CH_3). ^{13}C NMR (75 Hz, $CDCl_3$/pyridine-d_5): δ, ppm 168.3, 133.4, 129.6, 124.2, 30.4, 29.0, 22.1, 13.2. The other analytical data correspond to the data published in literature [10].

1,4,8,11,15,18,22,25-Octakis(pentan-3-yl)phthalocyanine (2H). The compound **2H** was prepared from **2Mg** (100 mg, 0.074 mmol) according to the general procedure for synthesis of metal-free derivatives. Mobile phase: chloroform/THF (30:1) (R_f = 0.72). Yield 77 mg (78%) of brown solid. UV-vis (THF): λ_{max}, nm (log ε) 802 (5.17), 716 (4.58), 515 (sh), 357 (4.67). ν_{max}/cm^{-1} 3304, 2964, 2931, 2872, 1559, 1460, 1377, 1278, 1225, 1197, 1136,

1091, 1044, 907. ^{1}H NMR (300 Hz, $CDCl_3$/pyridine-d_5): δ, ppm 7.95 (s, 8H, ArH), 3.81–3.63 (m, 8H, SCH), 2.25–1.95 (m, 32H, -SCHCH_2), 1.27 (t, J = 7 Hz, 48H, CH_3). ^{13}C NMR (75 Hz, $CDCl_3$/pyridine-d_5): δ, ppm 136.37, 133.62, 132.91, 130.87, 129.18, 127.02, 49.51, 27.03, 11.98. MS (MALDI): *m/z* 1330.5 $[M]^+$, 1353.47 $[M + Na]^+$.

1,4,8,11,15,18,22,25-Octakis(phenylsulfanyl) phthalocyanine (4H). The compound **4H** was prepared from **4Mg** (129 mg, 0.092 mmol) according to the general procedure for synthesis of metal-free derivatives. Mobile phase: toluene/THF (50:1) (R_f = 0.80). Yield 78 mg (61%) of brown solid. UV-vis (THF): λ_{max}, nm (log ε) 802 (4.87), 713 (4.30), 522 (sh), 356 (4.75). ^{1}H NMR (300 Hz, $CDCl_3$/pyridine-d_5): δ, ppm 8.03–7.80 (m, 16H, ArH), 7.57–7.41 (m, 24H, ArH), 7.31–7.22 (m, 8H, ArH). The other analytical data correspond to the data published in literature [11].

1,4,8,11,15,18,22,25-Octakis(2,6-dimethylphenylsulfanyl)phthalocyane (5H). The compound **5H** was prepared from **5Mg** (136 mg, 0.084 mmol) according to the general procedure for synthesis of metal-free derivatives. Mobile phase: toluene/hexane (1:1) (R_f = 0.33). Yield 100 mg (75%) of brown solid. UV-vis (THF): λ_{max}, nm (log ε) 817 (5.29), 725 (4.67), 536 (sh), 358 (4.77). ^{1}H NMR (300 Hz, $CDCl_3$/pyridine-d_5): δ, ppm 7.68–7.59 (m, 24H, ArH), 7.23 (s, 8H, ArH), 2.94 (s, 48H, CH_3). ^{13}C NMR (75 Hz, $CDCl_3$/pyridine-d_5): δ, ppm 144.5, 137.8, 133.5, 129.1, 128.3, 125.4, 125.2, 22.1. The other analytical data correspond to the data published in literature [12].

General procedure for synthesis of zinc* (II) *complexes. The metal-free derivative **1H**, **2H**, **4H** or **5H** (1 eq.) was dissolved in pyridine (15 mL) and anhydrous zinc acetate was added (7 eq.). The reaction mixture was heated at reflux for 2 h. Hereupon, the mixture was left to cool down and water (20 mL) was added. The precipitate was collected by filtration and thoroughly washed with water and methanol. The crude product was purified by column chromatography on silica (mobile phase is mentioned at each compound below).

1,4,8,11,15,18,22,25-Octakis(butylsulfanyl)phthalocyaninato zinc (II) (1Zn). The compound **1Zn** was prepared from **1H** (49 mg, 0.04 mmol) according to the general procedure for synthesis of zinc complexes. Mobile phase: chloroform (R_f = 0.10). Yield 45 mg (91%) of green solid. UV-vis (THF): λ_{max}, nm (log ε) 779 (5.17), 699 (4.57), 507 (sh), 359 (4.68). ^{1}H NMR (300 Hz, $CDCl_3$/pyridine-d_5): δ, ppm 7.76 (broad s, 8H, ArH), 3.31 (broad s, 16H, SCH_2), 2.1–1.89 (m, 16H, SCH_2CH_2), 1.82–1.61 (m, 16H, CH_2CH_3), 1.09 (t, J = 7 Hz, 24H, CH_3). ^{13}C NMR (75 Hz, CDCl3/pyridine-d_5): δ, ppm 138.24, 129.81, 128.72, 123.69, 31.02, 30.39, 22.12, 13.17. The other analytical data correspond to the data published in literature [10].

1,4,8,11,15,18,22,25-Octakis(pentan-3-yl)phthalocyaninato zinc (II) (2Zn). The compound **2Zn** was prepared from **2H** (50 mg, 0.038 mmol) according to the general procedure for synthesis of zinc complexes. Mobile phase: toluene (R_f = 0.65). Yield 37 mg (75%) of brown solid. UV-vis (THF): λ_{max}, nm (log ε) 777 (5.21), 697 (4.59), 510 (sh), 344 (4.62). ^{1}H NMR (300 Hz, $CDCl_3$/pyridine-d_5): δ, ppm 7.81 (s, 8H, ArH), 3.56 (quint, J = 6 Hz, 8H, SCH), 2.01–1.81 (m, 32H, $SCHCH_2$), 1.10 (t, J = 7 Hz, 48H, CH_3). ^{13}C NMR (75 Hz, $CDCl_3$/pyridine-d_5): δ, ppm 152.0, 131.7, 125.4, 48.7, 26.0, 11.0. The other analytical data corresponded to the data published in literature [20].

1,4,8,11,15,18,22,25-Octakis(phenylsulfanyl) phthalocyaninato zinc (II) (4Zn). The compound **4Zn** was prepared from **4H** (78 mg, 0.056 mmol) according to the general procedure for synthesis of zinc complexes. Mobile phase: toluene/THF (50:1) (R_f = 0.33). Yield 67 mg (82%) of green solid. UV-vis (THF): λ_{max}, nm (log ε) 779 (5.27), 695 (4.66), 497 (sh), 352 (4.76). ^{1}H NMR (300 Hz, $CDCl_3$/pyridine-d_5): δ, ppm 7.98–7.83 (m, 16H, ArH), 7.52–7.41 (m, 24H, ArH), 7.31–7.25 (m, 8H, ArH). ^{13}C NMR (75 Hz, $CDCl_3$/pyridine-d_5): δ, ppm 153.7, 134.1, 134.0, 133.0, 129.9, 129.0, 127.2. The other analytical data correspond to the data published in literature [12].

1,4,8,11,15,18,22,25-Octakis(2,6-dimethylphenylsulfanyl)phthalocyaninato zinc (II) (5Zn). The compound **5Zn** was prepared from **5H** (59 mg, 0.37 mmol) according to the general procedure for synthesis of zinc complexes. Mobile phase: toluene/THF (50:1) (R_f = 0.49). Yield 48 mg (78%) of brown solid. UV-vis (THF): λ_{max}, nm (log ε) 793 (5.36), 706 (4.71) 511 (sh), 354 (478). ^{1}H NMR (300 Hz, $CDCl_3$/pyridine-d_5): δ, ppm 7.40–7.20 (m, 24H, ArH), 6.94–6.86 (s, 8H, ArH), 2.63 (s, 48H, CH_3). ^{13}C NMR (75 Hz, $CDCl_3$/pyridine-d_5): δ, ppm 153.9, 144.5, 134.4, 132.6, 131.1, 129.5, 129.2, 128.9, 128.4, 124.6, 22.2. IR: ν_{max}, cm^{-1} 3052, 2955, 2920, 2853, 2730, 2457, 1933, 1879, 1771, 1731, 1603, 1558, 1489, 1376, 1319, 1212, 1166, 1137, 1112, 1053, 914, 169. MS (MALDI): *m/z* 1664.2 $[M]^+$.

Fluorescence measurements

All of the samples were re-purified using preparative TLC prior the measurement to ensure high purity of the samples (mobile phases are mentioned in Experimental part). All of the emission spectra were corrected for the instrument response. The fluorescence quantum yields (Φ_F) were determined in THF *via* the comparative method using unsubstituted zinc phthalocyanine (ZnPc) as a reference (Φ_F = 0.32 in THF [25]). Both the reference and sample were excited at 360 nm. The absorbance at the Q-band maximum was maintained below 0.05 to limit the inner filter effect. The value of Φ_F was calculated using Equation 1 [26]:

$$\Phi_F^S = \Phi_F^S \frac{F^S}{F^R}\left(\frac{1-10^{-A^R}}{1-10^{-A^S}}\right) \quad (1)$$

where F is the integrated area under the emission spectrum and A is the absorbance at the excitation wavelength.

The superscripts *R* and *S* correspond to the reference and sample, respectively. All of the experiments were performed in triplicate with the reported data representing the mean (estimated error ±15%).

Determination of the singlet oxygen production

All of the samples were re-purified using preparative TLC prior to the measurement to ensure high purity of the sample (mobile phases are mentioned in Experimental part). The quantum yields of the singlet oxygen (Φ_Δ) were determined in THF according to a previously published procedure [27] using the decomposition of a chemical trap 1,3-diphenylisobenzofuran (DPBF) with ZnPc as a reference ($\Phi_\Delta = 0.53$ in THF [28]). The detailed procedure was as follows: 2.5 mL of a DPBF stock solution in THF (5×10^{-5} M) was transferred into a 10 mm × 10 mm quartz optical cell and saturated with oxygen for 1 min. Then, a stock solution of the tested compound in THF (typically 20 μL) was added to achieve an absorbance of the final solution in the Q-band maximum of approximately 0.1. The solution was stirred and irradiated using a xenon lamp (100 W, ozone-free XE DC short-arc lamp, Newport). The incident light was filtered through a water filter (6 cm) and an OG530 cut-off filter (Newport) to remove the heat and light below 523 nm, respectively. A decrease of DPBF in the solution as a function of the irradiation time was monitored at 414 nm. All of the experiments were performed in triplicate, and the data presented herein represent the mean of the three experiments (estimated error: ±15%).

Protonation of azomethine nitrogens

A stock solution (2 mL) of **1Zn**, **2Zn**, **4Zn**, **5Zn** or **6Zn** (c = 1 μM) in THF was transferred into the 10 × 10 mm quartz optical cell and absorption spectrum was recorded. Then, defined amounts (typically 10 or 50 μL) of trifluoroacetic acid (TFA) were added and absorption spectra were measured after each addition. The final concentration of TFA in the sample ranged from 0.0005% to 21.5% (v/v) (that corresponds to 0.00065–2.82 M). Trituration of TFA (0.1 mL TFA in 9.9 mL THF) was employed in some cases to reach required low concentration of TFA in the sample. Finally, tetrabutylammonium hydroxide (TBAH) in THF (c = 100 mM) (10 or 50 μL) was added to the sample at the maximum of the mono-protonated form to confirm the reversibility. The presented data were corrected for dilution. Data are presented by plotting the absorbance at Q-band maximum as a function of the TFA concentration. The association constant K was calculated from the plotted data using nonlinear regression in Prism 6 for Windows (GraphPad Software, Inc.).

Photostability

A stock solution (2.5 mL) of **1Mg–6Mg** (c = 2 μM) in THF was transferred into the 10 × 10 mm quartz optical cell, stirred at room temperature and irradiated for total time 20 min by using halogen lamp (EMOS, 400 W). The electronic absorption spectra were measured at defined irradiation time (typically in 5 min periods). The incident light was filtered through a water filter (65 mm) to remove the heat from the light source. The decomposition of a sample was expressed as a relative decrease of its absorbance at Q-band maximum in time. All measurements were performed three times and presented data represent mean of these three experiments. Simultaneously, control solutions of **1Mg–6Mg** were measured under the same conditions in the dark. No changes in electronic absorption spectra of control solutions were observed without irradiation.

RESULTS AND DISCUSSION

Synthesis

In general, synthesis of Pcs is performed by cyclotetramerization of precursors, usually substituted phthalonitriles. The precursors **2**, **3**, **4** and **7** (see Scheme 1) were prepared *via* nucleophilic substitution according to the previously published procedures [12, 20–22]. In these cases, 2,3-dicyano-1,4-phenylene bis(4-methylbenzenesulfonate) (**8**) [23] and appropriate alkylthiolate or arylthiolate reacted in the presence of K_2CO_3 as a base to give required products in reasonable yields 34–66%. Thiols needed for the nucleophilic substitution were commercially available besides 1-adamantanethiol which was prepared from 1-bromoadamantane according to the reported procedure [29].

Methods described in literature for synthesis of precursors **1** [10] and **5** [12] suffered from low yields, thus, the reaction conditions were optimized. Regarding precursor **1**, tosyl leaving group (*i.e.* compound **8** as a starting material) was used instead of triflate leaving group in 1,2-dicyano-3,6-bis(trifluorosulfonyl)benzene to improve the yield from published 19% up to 59%. In the case of precursor **5**, we were not able to achieve the 53% yield employing the published procedure. Thus, various reaction conditions were tested such as different bases (K_2CO_3, NaOH, CsF), reaction temperatures (-12 °C, room temperature, up to reflux), reaction times (3–60 h), solvents (THF, DMSO), and air/inert atmosphere. The best yields were obtained in combination of K_2CO_3, anhydrous DMSO, argon atmosphere and room temperature where the yield was improved up to 74%.

Synthesis of metal-free derivatives **1H** [10], **3H** [19], **4H** [11], **5H** [12], were reported in literature and were based on lithium assisted cyclotetramerization in alcohols. However, magnesium and zinc complexes were also the subjects of interest in this study. Therefore, cyclotetramerization of **1**–**5** was performed with magnesium butoxide as an initiator of the reaction leading to the formation of magnesium complexes **1Mg–5Mg**.

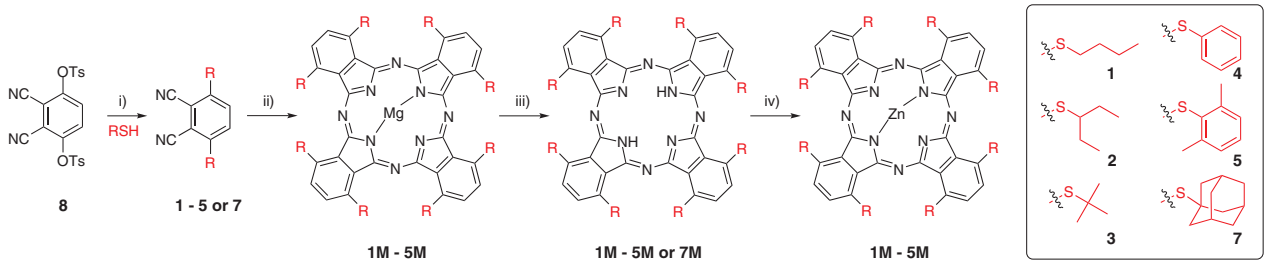

Scheme 1. Synthetic pathway for target compounds. (i) K_2CO_3, DMSO, rt, 16 h. (ii) $Mg(OBu)_2$, BuOH, I_2, reflux, 24 h. (iii) TsOH, THF, rt, 30 min. (iv) $Zn(OAc)_2$, pyridine, 60 min

Generally, the magnesium cation can be released from the center of Pcs under acidic solution. Thus, treatment of magnesium complexes with *p*-toluenesulfonic acid (TsOH) afforded the metal-free derivatives **1H**, **2H**, **4H** and **5H**. Finally, the zinc complexes **1Zn** [10], **2Zn** [20], **4Zn** and **5Zn** were synthesized from the corresponding metal-free derivatives by the reaction with zinc acetate (Scheme 1). This reaction sequence reduced the tedious purification after cyclotetramerization to one (purification of magnesium complexes). The metal exchange procedures proceeded in high yields with limited amount of side products that were easily removed. The treatment of **3Mg** with TsOH or trifluoroacetic acid (TFA) caused rapid decomposition of the macrocycle and no product formation was registered. Missing stabilization effect of central cation together with the pronounced steric hindrance of *tert*-butylsulfanyl groups leading to the extreme distortion of the macrocycle may be the reason for the instability of such macrocycle. Indeed, low stability of **3H** has been recently pointed out in literature by the authors who succeeded in isolation of this unstable and strongly distorted macrocycle [19]. As a consequence, **3H** was not prepared despite the fact that different methods were tried (removal of central magnesium under acidic conditions, direct cyclotetramerization using LiOBu as the initiator, *etc*.) even considering the method that was recently reported. Also, direct synthesis of **3Zn** *via* metal cation template effect with zinc acetate in anhydrous pyridine or quinoline was not successful. Traces of **3Zn** were obtained using cyclotetramerization in butanol with catalytic amount of DBU and anhydrous zinc acetate. The structure could not be unequivocally confirmed and only absorption spectrum was taken. The position of Q-band at 721 nm in THF (see Fig. S2) was comparable with **3Mg** (724 nm, see Table 1) suggesting, thus, proper product. Due to the missing analytical data, this compound was not included in further photophysical studies.

All attempts to cyclotetramerize precursor **7** bearing bulky 1-adamantylsulfanyl groups either with magnesium butoxide in butanol or magnesium octanoxide in octanol failed to produce the desired product. Cyclotetramerization in butanol with anhydrous zinc acetate and butoxide generated by DBU was not successful as well. The template method using anhydrous zinc acetate in high boiling solvent (quinoline, DMF) also failed and only dark decomposition products were observed. Lithium butoxide is known as the strongest initiator of the cyclotetramerization, however, only traces of presumably metal-free product were detected by UV/vis absorption spectrum in the reaction mixture with the Q-band maximum in expected area (Fig. S1). Nevertheless, the structure could not be confirmed, thus, this compound was not discussed in the following parts of the paper. Extreme bulkiness of adamantyl that is even bigger than *tert*-butyl most likely produced macrocycle with even lower stability than for **3H**.

Absorption spectra

The electronic absorption spectra of all target macrocycles were measured in THF and the obtained data are summarized in Table 1 and Fig. 1. The absorption spectra of metal complexes had typical high energy B-bands ranging from 340 nm to 430 nm and low energy Q-bands in range from 724 nm to 793 nm. The sharp and unsplit Q-bands of all investigated compounds indicated that only monomeric species are present in solution without any aggregates. As obvious from Fig. 1, extinction coefficients were directly proportional to the red-shift of Q-band ranging for example for magnesium complexes from 120 000 $M^{-1}.cm^{-1}$ (λ_{max} at 724 nm) up to 240 000 $M^{-1}.cm^{-1}$ (λ_{max} at 788 nm). In accordance with non-peripheral Pcs published in literature [10], Q-bands of all target compounds (besides **3Mg**, that was specific, see below) were significantly shifted to the red (approx. of 70 nm) in comparison to similar peripherally substituted Pcs (see Table 1). The Q-band positions in the series of magnesium complexes appeared at 724 nm (*tert*-butylsulfanyl, **3Mg**) $<<$774 nm (pentan-3-ylsulfanyl, **2Mg**) ~775 nm (phenylsulfanyl, **4Mg**) ~776 nm (butylsulfanyl, **1Mg**) $<$788 nm (2,6-dimethylphenylsulfanyl, **5Mg**) (Fig. 1, Table 1). The position of the Q-band of both alkylsulfanyl and phenylsulfanyl substituents was similar leading to suggestion of limited effect of phenyl ring on the electronic structure. This is in agreement with conclusions reported recently for metal-free **4H** [11]. More bulky **5Mg** was red-shifted for more than 10 nanometers in comparison

Table 1. Absorption and photophysical data of investigated compounds in THF at room temperature[a]

Cpd.	Substitution	Central metal	λ_{max}, nm	λ_{em}, nm	$\Delta\lambda$, cm^{-1}	Φ_F [b]	Φ_Δ [b]	K, M^{-1}
1	-SBu	Mg	776	801	402	0.13	0.49	
		2H	805	840	517	0.048	0.052	
		Zn	779	806	430	0.069	0.75	513
2	-S(pentan-3-yl)	Mg	774	802	451	0.10	0.51	
		2H	802	840	564	0.032	0.096	
		Zn	777	804	432	0.053	0.76	493
3	-S*t*Bu	Mg	724	758	620	0.10	0.47	
4	-SPh	Mg	775	799	388	0.17	0.47	
		2H	802	834	478	0.061	0.064	
		Zn	779	804	399	0.080	0.74	6.11
5	-S(2,3-Me_2)Ph	Mg	788	805	268	0.12	0.48	
		2H	817	845	406	0.064	0.049	
		Zn	793	812	295	0.076	0.74	9.34
6 [25]	-S*t*Bu	Mg	699	709	202	0.23	0.23	
		Zn	697	707	203	0.16	0.68	0.53

[a]Absorption maximum at Q-band (λ_{max}), emission maximum (λ_{max}), stokes shift ($\Delta\lambda$), quantum yield of singlet oxygen production (Φ_Δ), quantum yield of florescence (Φ_F), association constant of reaction with TFA in THF (K). [b]Mean of three independent measurements, estimated error ±15.

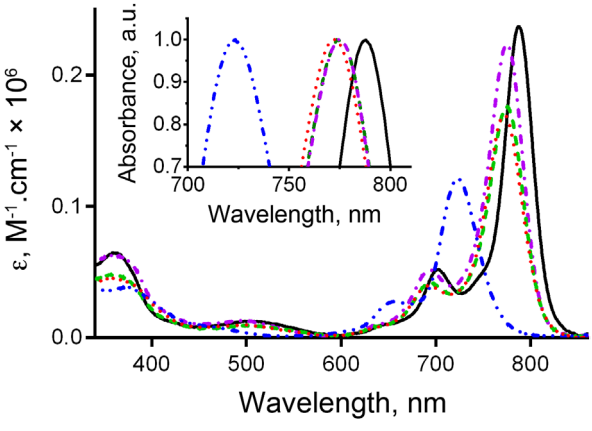

Fig. 1. Electronic absorption spectra (1 μM) of **1Mg** (green dashed line), **2Mg** (red dotted line), **3Mg** (blue double dot-dashed line), **4Mg** (purple dot-dashed line) and **5Mg** (black full line) in THF. Inset: enlarged Q-band area of normalized absorption spectra

to **4Mg**. Origin of the shift may have two explanation. The more bulky 2,6-dimethylphenyl substituent may lead to slightly more distorted macrocycle than in case of **4Mg**. The distortion of the Pc ring in non-peripherally substituted derivatives was reported several times to lead to small bathochromic shift [11, 15]. Alternatively, the pushing effect of methyls in *ortho* positions may contribute to a small red shift. Unexpectedly, significant hypsochromic shift of absorption maxima of **3Mg** of 52 nm in comparison to **1Mg** was observed and does not correspond with the distortion effect leading to small red-shift reported often in literature. This effect may be attributed to extreme distortion of the Pc macrocycle caused by steric hindrance of bulky *tert*-butyl substituents. The extreme distortion of metal-free Pc with the same substitution (**3H**) was recently demonstrated by X-ray structure, and the hypsochromic shift of its Q-band maximum (750 nm in THF, *i.e.* shift of 55 nm compared to hexylsulfanyl derivative) was explained to be due to decreased conjugation potency of the benzo rings to the central pyrrolic rings [19]. Interestingly, the reported blue shift of 55 nm between *tert*-butylsulfanyl and hexylsulfanyl derivatives in metal-free Pcs is exactly the same as the blue shift observed in our series in magnesium Pcs substituted with *tert*-butylsulfanyl (**3Mg**) and butylsulfanyl (**1Mg**) indicating similarly decreased conjugation.

The similar dependences described above for magnesium complexes were observed also for zinc and metal-free derivatives (Figs S1 and S2). Considering the metal-free derivatives, they had the absorption maxima over 800 nm with sharp unsplit shape of Q-band. Despite the loss of macrocycle symmetry due to presence of central hydrogens, unsplit character of spectra is typical for metal-free Pcs absorbing in near-infrared region [11].

Fluorescence and singlet oxygen quantum yields

Fluorescence emission and singlet oxygen production were studied in THF because of good solubility and

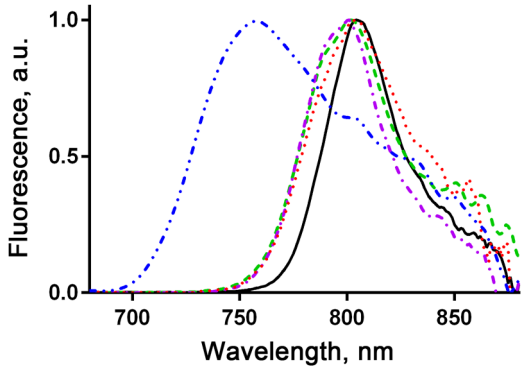

Fig. 2. Normalized emission spectra of **1Mg** (green dashed line), **2Mg** (red dotted line), **3Mg** (blue double dot-dashed line), **4Mg** (purple dot-dashed line) and **5Mg** (black full line) in THF. Spectra are corrected for the instrument response

non-aggregating behavior of target compounds in this solvent. The quantum yields of fluorescence (Φ_F) and singlet oxygen quantum yields (Φ_Δ) were determined using unsubstituted zinc phthalocyanine (ZnPc, $\Phi_{F(THF)}$ = 0.32 [25] and $\Phi_{\Delta(THF)}$ = 0.53 [28]) as a reference. The shape of the emission spectra were typical for Pcs with a small Stokes shift (Figs 2 and S3). The excitation spectra were also recorded and they perfectly mirrored the absorption spectra which proves only monomeric forms of Pcs in the solution without presence of any aggregates (Figs S4 and S5). Thus, the Φ_F and Φ_Δ determination was not affected by aggregation at all. The obtained data are summarized in the Table 1. The different substitution of target compounds within the series did not significantly affected photophysical properties and the values of Φ_F and Φ_Δ differed only in relation to the central metal following the rule of heavy atom effect [30]. According to this rule, the presence of heavy atoms in the molecule increases the probability by which the compound undergoes intersystem crossing that leads to the higher singlet oxygen production and a concomitant decrease of other competitive relaxation pathways, *e.g.* fluorescence emission. Therefore, magnesium complexes **1Mg–5Mg** reached values of Φ_F in the range of 0.10–0.17 while zinc complexes in the range of 0.053–0.080 only. Regarding Φ_Δ, zinc complexes of target Pcs possessed higher values (0.74–0.76) than their corresponding magnesium derivatives (0.47–0.51). Interestingly, the strong steric distortion of **3Mg** macrocycle did not influence significantly the photophysical properties that were fully comparable with other magnesium complexes in the series. In comparision to corresponding peripherally substituted Pc (*i.e.* **6Zn**), it was obvious that shifting the substituent to the non-peripheral positions caused significant improvement of singlet oxygen production (**6Zn** of Φ_Δ is 0.65 only) on the account of fluorescence emission (Φ_F of **6Zn** is 0.28). Metal-free Pcs usually dissipate energy also by different pathways [25, 31, 32], thus, their Φ_F and Φ_Δ were significantly lower in comparison to metal complexes.

Protonation of azomethine nitrogens

The protonation of azomethine nitrogens is usually deduced from the typical changes in electronic

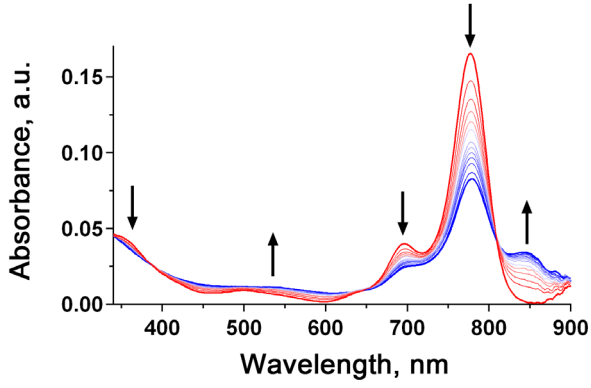

(a)

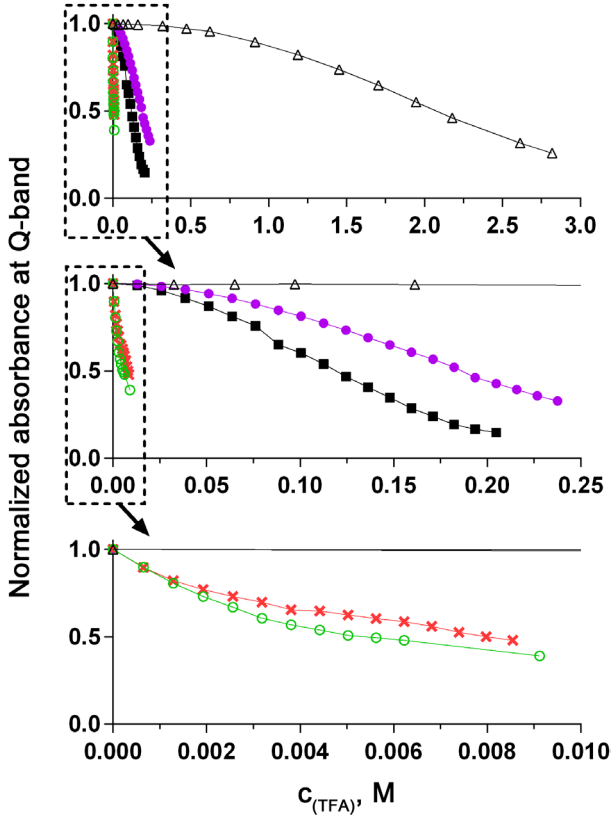

(b)

Fig. 3. (a) Changes in absorption spectra of **2Zn** in THF (1 μM) after addition of TFA. Spectra are corrected for dilution; (b) Decrease of absorbance at Q-band maxima of **1Zn** (green full line, open circle), **2Zn** (red full line, cross), **4Zn** (purple full line, full circle), **5Zn** (black full line, full square) and **6Zn** (black dashed line, open triangle) in THF (1 μM) after stepwise addition of TFA. Absorbance at Q-band was normalized to be one for each sample solution without TFA

absorption spectra such as decrease of Q-band maximum and formation of a new red-shifted band [33, 34]. The zinc complexes were chosen for the purposes of this study because magnesium complexes may undergo undesirable demetalation under acidic conditions. Compound **6Zn** was introduced into the study to enable comparison with similarly peripherally substituted Pc. Stepwise addition of TFA into the THF solution of studied compounds led to decrease of Q-band maximum with concomitant increase of absorption close to 900 nm (Figs 3a and S6). Unfortunately, the formation of the new red-shifted band could not be optimally studied due to the limitation of instrument. However, presence of several isosbestic points in the spectra clearly confirmed the formation of mono-protonated form from non-protonated one and also showed that the decrease of Q-band maximum was not caused by decomposition of the sample but can be attributed solely to the protonation of azomethine nitrogens atom. Finally, tetrabutylammonium hydroxide was always added into the solution of mono-protonated form of studied compounds leading to the restoration of original Q-band shape. This fact confirmed reversibility of the whole process without decomposition.

Absorbance in Q-band maximum during titration was plotted as a function of acid concentration (Fig. 3b) and association constants (K) of Pcs reaction with TFA in THF were calculated (Table 1). As obvious from Fig. 3b and K values, basicity of the azomethine nitrogens was found to be extremely different within the series. The strongest basicity was observed for alkylsulfanyl derivatives **1Zn** and **2Zn** with K in a range of ~500 M^{-1}. Steric effects in arylsulfanyl derivatives **4Zn** and **5Zn** are a likely cause of somewhat lower basicity of their azomethine nitrogens with K in the range of ~10 M^{-1} that is, however, still far above the basicity of the nitrogens in peripherally substituted **6Zn** with K = 0.53 M^{-1}. Increased basicity of non-peripherally substituted Pcs over the peripherally substituted ones has already been noted in literature [4, 34]. In particular, for alkyloxy derivatives it was explained by stabilization of the protonated forms by intramolecular hydrogen bonds between proton attached to the azomethine nitrogen and either oxygen [34]. Although the hydrogen bonding is not expected with the sulfur atoms, the distance between the sulfurs in adjacent units of non-peripherally substituted Pcs has been reported to be close to twice the van der Waals radius [12] of the chalcogen and that is why the van der Waals interaction may stabilize the azomethine protonated form. Such interaction is obviously missing in peripherally substituted Pcs. On the other hand, different basicity of present series can be the result of different distortion of the macrocycle. Indeed, substantially increased basicity of nitrogens in highly distorted non-peripherally octaphenyl substituted metal-free and zinc Pcs has been reported [34, 35]. However, clear evidence for presented compounds cannot be given now. Evidently,

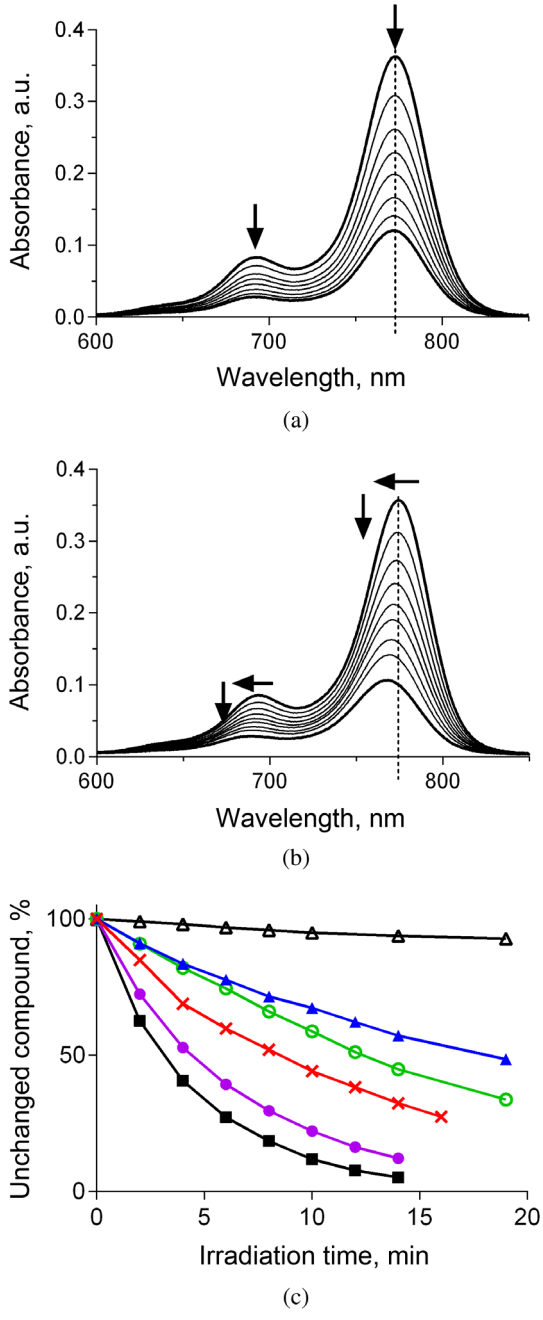

Fig. 4. Changes in absorption spectra after light irradiation of (a) **2Mg** and (b) **1Mg** in THF (2 μM) at rt; (c) Photostability of **1Mg** (green full line, open circle), **2Mg** (red full line, cross), **3Mg** (blue full line, full triangle), **4Mg** (purple full line, full circle), **5Mg** (black full line, full square) and **6Mg** (black dashed line, open triangle) after light irradiation (EMOS, 400 W) in THF at rt

the definite explanation of different basicity of target Pcs is challenging and needs to be studied further.

Photostability

Photobleaching of Pcs and related compounds upon light irradiation is a well-known undesirable feature.

Decomposition of **1Mg–5Mg** on light was observed even during synthesis and storing the samples that was why the products were kept in the dark. The extent of photobleaching was studied in THF by the mean of absorption spectroscopy. Compound **6Mg** was introduced into the study to compare the photostability of non-peripherally substituted Pcs with similar peripherally substituted Pc. The significant decrease of absorbance at all wavelength without any new-band formation was observed after irradiation in almost all cases (Figs 4a and S7) suggesting full decomposition of the macrocycles to small molecules. Only in the case of **1Mg**, the decrease in Q-band maximum was accompanied by its blue shift for 10 nm (Figs 4b and S7a). Considering the fact that alkylsulfonyl Pcs are typically blue shifted in comparison to alkylsulfanyl Pcs [36], this blue shift in **1Mg** during decomposition can be attributed to oxidation of thioethers to alkylsulfinyl and alkylsulfonyl groups. This was detected only for the Pc with the least sterically demanding substituent (*n*-butylsulfanyl) indicating that the photooxidation of the thioether linkage in Pcs is inhibited by more bulky substituents. The decrease of absorbance in the Q-band maximum was subsequently plotted as a function of time and is depicted in Fig. 4c. Non-peripherally substituted Pcs proved to be less stable than peripherally substituted **6Mg**. The photostability increased in series **5Mg** < **4Mg** < **2Mg** < **1Mg** < **3Mg** ⩽ **6Mg**. These data are in accordance with the literature, where macrocycles absorbing at higher wavelengths are usually less photostable [14, 15]. Arylsulfanyl substituted Pcs showed more pronounced decomposition upon light exposer than the alkylsulfanyl as almost complete decomposition of the macrocycles **4Mg** and **5Mg** was observed within less than 15 min of irradiation. The control samples of **1Mg–6Mg** kept under the same conditions but in the dark showed no change in their absorption spectra.

CONCLUSION

A series of magnesium, zinc and metal-free non-peripherally alkylsulfanyl and arylsulfanyl substituted Pcs was prepared and their spectral and photophysical properties were studied. Their properties (*i.e.* position of Q-band maximum, Φ_Δ and Φ_F, basicity of azomethine nitrogens, photostability) were compared within the series as well as discussed in comparison with similar peripherally substituted Pcs.

In accordance with literature data, the shifting of the substituents from peripheral to non-peripheral positions of Pc caused ~70 nm red-shift of Q-band. However, unexpected blue shift of approximately 50 nm was observed for **3Mg** bearing extremely bulky *tert*-butylsulfanyl substituents compared to **1Mg** bearing *n*-butylsulfanyl groups. This interesting phenomenon contradicts the well-known widely described knowledge of shifting the absorption maximum to the red part of the spectrum due to increased distortion of the macrocycle [11, 12, 16]. In the case of **3Mg**, the extreme distortion of the macrocycle disrupted probably the π-electron system of the macrocycle similarly as published recently by Dumoulin at co-workers for the corresponding metal-free Pc [19].

Bulkiness and the type of non-peripheral substituent (alkylsulfanyl *vs.* arylsulfanyl) did not affect the photophysical properties such as quantum yields of singlet oxygen production and fluorescence emission and the values of Φ_Δ and Φ_F differed only in respect to the central metal following the rule of heavy atom effect. Interestingly, Φ_Δ values of non-peripherally substituted Pcs reached significantly higher values than for similar peripherally substituted Pcs that make them promising candidates to be used as photosensitizers in photodynamic therapy. However, the choice of a properly bulky non-peripheral substituent should be considered to achieve desirable red shift of absorption maxima and diminish aggregation, but concurrently to avoid excessive distortion of macrocycle, which could cause reverse hypsochromic spectral shift.

The basicity of azomethine nitrogens was clearly dependent on the position and also the character of substituent. Thus, non-peripherally substituted Pcs showed increased basicity than similar peripherally substituted ones with *K* values in THF higher for several orders of magnitude. Furthermore, the basicity was even more pronounced at alkylsulfanyl derivatives than arylsulfanyl most likely due to steric effects.

The target compounds were shown to be more prone to photodecomposition than corresponding peripherally substituted Pc with the pronounced decomposition at arylsulfanyl derivatives.

Acknowledgements

This work was supported by Czech Science Foundation (No. 13-27761S) and Charles University in Prague (SVV 260 183). The authors would like to thank Jiří Kuneš for the NMR measurements, and Juraj Lenčo for the MALDI-TOF MS measurements.

Supporting information

Figures S1–S7 are given in the supplementary material. This material is available free of charge *via* the Internet at http://www.worldscinet.com/jpp/jpp.shtml.

REFERENCES

1. Sharman WM, Allen CM and van Lier JE. *Drug Discovery Today* 1999; **4**: 507–517.
2. Moan J and Peng Q. *Anticancer Res.* 2003; **23**: 3591–3600.
3. Rosenthal I. *Photochem. Photobiol.* 1991; **53**: 859–870.

4. Derkacheva VM, Kaliya OL and Lukyanets EA. *Zh. Obsh. Khim.* 1983; **53**: 188–192.
5. Campbell WM, Jolley KW, Wagner P, Wagner K, Walsh PJ, Gordon KC, Schmidt–Mende L, Nazeeruddin MK, Wang Q, Gräzel M and Officer DL. *J. Phys. Chem. C* 2007; **111**: 11760–11762.
6. Bouvet M. *Anal Bioanal. Chem.* 2006; **384**: 366–373.
7. Hohnholz D, Steinbrecher S and Hanack M. *J. Mol. Struct.* 2000; **521**: 231–237.
8. Lv F, He XJ, Wu L and Liu TJ. *Bioorg. Med. Chem. Lett.* 2013; **23**: 1878–1882.
9. Cook MJ, Dunn AJ, Howe SD, Thomson AJ and Harrison KJ. *J. Chem. Soc., Perkin Trans.* 1 1988; 2453–2458.
10. Kobayashi N, Ogata H, Nonaka N and Luk'yanets EA. *Chem.-Eur. J.* 2003; **9**: 5123–5134.
11. Kobayashi N, Furuyama T and Satoh K. *J. Am. Chem. Soc.* 2011; **133**: 19642–19645.
12. Furuyama T, Satoh K, Kushiya T and Kobayashi N. *J. Am. Chem. Soc.* 2014; **136**: 765–776.
13. Guo LQ, Ellis DE, Hoffman BM and Ishikawa Y. *Inorg. Chem.* 1996; **35**: 5304–5312.
14. Cook MJ, Chambrier I, Cracknell SJ, Mayes DA and Russell DA. *Photochem. Photobiol.* 1995; **62**: 542–545.
15. Chambrier I, Cook JM and Wood PT. *Chem. Commun.* 2000: 2133–2134.
16. Fukuda T, Homma S and Kobayashi N. *Chem.-Eur. J.* 2005; **11**: 5205–5216.
17. Machacek M, Cidlina A, Novakova V, Svec J, Rudof E, Miletin M *et al*. *J. Med. Chem.* 2015; **58**: 1736–1749.
18. George RD, Snow AW, Shirk JS and Barger WR. *J. Porphyrins Phthalocyanines* 1998; **2**: 1–7.
19. Zorlu Y, Kumru U, Isci U, Divrik B, Jeanneau E, Albrieux F *et al*. *Chem. Commun.* 2015; **51**: 6580–6583.
20. Suchanek J, Lang K, Novakova V, Zimcik P, Zelinger Z and Kubat P. *Photochem. Photobiol. Sci.* 2013; **12**: 743–750.
21. Kumru U, Dumoulin F, Jeanneau E, Yuksel F, Cabezas Y, Zorlu Y and Ahsen V. *Struct. Chem.* 2012; **23**: 175–183.
22. Zorlu Y, İşci Ü, Ün İ, Kumru U, Dumoulin F and Ahsen V. *Struct. Chem.* 2013; **24**: 1027–1038.
23. Mbambisa G, Tau P, Antunes E and Nyokong T. *Polyhedron* 2007; **26**: 5355–5364.
24. Kostka M, Zimcik P, Miletin M, Klemera P, Kopecky K and Musil Z. *J. Photochem. Photobiol., A* 2006; **178**: 16–25.
25. Zimcik P, Novakova V, Kopecky K, Miletin M, Uslu Kobak RZ, Svandrlikova E *et al*. *Inorg. Chem.* 2012; **51**: 4215–4223.
26. Lakowicz JR. *Principles of Fluorescence Spectroscopy*, 3rd ed., New York: Springer, 2006.
27. Musil Z, Zimcik P, Miletin M, Kopecky K, Link M, Petrik P and Schwarz J. *J. Porphyrins Phthalocyanines* 2006; **10**: 122–131.
28. Kaestner L, Cesson M, Kassab K, Christensen T, Edminson PD, Cook MJ *et al*. *Photochem. Photobiol. Sci.* 2003; **2**: 660–667.
29. Girard P, Guillot N, Motherwell WB, Hay-Motherwell RS and Potier P. *Tetrahedron* 1999; **55**: 3573–3584.
30. McClure DS. *J. Chem. Phys.* 1949; **17**: 905–913.
31. McVie J, Sinclair RS and Truscott TG. *J. Chem. Soc., Faraday Trans.* 2 1978; **74**: 1870–1879.
32. *Handbook of Porphyrin Science*, Kadish KM, Smith KM and Guilard R. (Eds.) World Scientific Publishing: Singapore, 2010.
33. Beeby A, FitzGerald S and Stanley CF. *J. Chem. Soc., Perkin Trans. 2* 2001: 1978–1982.
34. Fukuzumi S, Honda T and Kojima T. *Coord. Chem. Rev.* 2012; **256**: 2488–2502.
35. Honda T, Kojima T, Kobayashi N and Fukuzumi S. *Angew. Chem., Int. Ed.* 2011; **50**: 2725–2728.
36. Zhang Y, Ma P, Zhu PH, Zhang XY, Gao YN, Qi DD *et al*. *J. Mater. Chem.* 2011; **21**: 6515–6524.